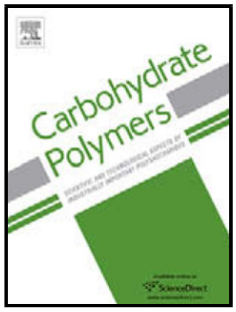

Title: Lubrication of starch in Ionic liquid-water mixtures: soluble carbohydrate polymers form a boundary film on hydrophobic surfaces.

Author: Gleb E. Yakubov Lei Zhong Ming Li Michael W. Boehm Fengwei Xie David A. Beattie Peter J. Halley Jason R. Stokes

PII: S0144-8617(15)00605-0
DOI: http://dx.doi.org/doi:10.1016/j.carbpol.2015.06.087
Reference: CARP 10078

To appear in:

Received date: 25-5-2015
Revised date: 18-6-2015
Accepted date: 29-6-2015

Please cite this article as: Yakubov, Gleb E., Zhong, Lei., Li, Ming., Boehm, Michael W., Xie, Fengwei., Beattie, David A., Halley, Peter J., & Stokes, Jason R., Lubrication of starch in Ionic liquid-water mixtures: soluble carbohydrate polymers form a boundary film on hydrophobic surfaces.*Carbohydrate Polymers* http://dx.doi.org/10.1016/j.carbpol.2015.06.087

Lubrication of starch in Ionic liquid-water mixtures: soluble carbohydrate polymers form a boundary film on hydrophobic surfaces.

Gleb E. Yakubov [1,2*], Lei Zhong [3,4], Ming Li [5], Michael W. Boehm [2†], Fengwei Xie [3], David A. Beattie [6], Peter J. Halley [2,3], Jason R. Stokes [1,2]

1- Australian Research Council Centre of Excellence in Plant Cell Walls, The University of Queensland, Brisbane, QLD 4072, Australia
2- School of Chemical Engineering, The University of Queensland, Brisbane, QLD 4072, Australia
3- Australian Institute for Bioengineering and Nanotechnology, The University of Queensland, Brisbane, QLD 4072, Australia
4- Key Laboratory of Chemical and Biological Transformation Processes, School of Chemistry and Chemical Engineering, Guangxi University for Nationalities, Nanning 530006, China
5- Centre for Nutrition and Food Sciences, Queensland Alliance for Agriculture and Food Innovation, The University of Queensland, Brisbane, QLD 4072, Australia
6- Ian Wark Research Institute, University of South Australia, Mawson Lakes Campus, Mawson Lakes, SA 5095

† - current address Micro/Bio/Nanofluidics Unit, Okinawa Institute of Science and Technology Graduate University, Okinawa 904-0495, Japan

* - Corresponding author gleb.yakubov@uq.edu.au

Highlights

 Soluble starch polymers enhance lubrication of ionic liquid-water solvents A fraction of starch is highly soluble in 1-ethyl-3-methylimidazolium acetate Small amount of soluble starch reduces the boundary friction coefficient This low-friction is associated with a nanometre thick film formed from the amylose The presence of dissolved amylose enhances the lubrication of starch suspensions

Abstract

Soluble starch polymers are shown to enhance the lubrication of ionic liquid-water solvent mixtures in low-pressure tribological contacts between hydrophobic substrates. A fraction of starch polymers

become highly soluble in 1-ethyl-3-methylimidazolium acetate (EMIMAc)-water solvents with ionic liquid fraction ≥ 60 wt%. In 65wt% EMIMAc, a small amount of soluble starch (0.33 wt%) reduces the boundary friction coefficient by up to a third in comparison to that of the solvent. This low-friction is associated with a nanometre thick film (ca. 2 nm) formed from the amylose fraction of the starch. In addition, under conditions where there is a mixture of insoluble starch particles and solubilised starch polymers, it is found that the presence of dissolved amylose enhances the lubrication of starch suspensions between roughened substrates. These findings open up the possibility of utilising starch biopolymers, as well as other hydrocolloids, for enhancing the performance of ionic liquid lubricants.

Keywords

Starch; Lubrication; Ionic Liquid; Amylose; Boundary Friction; Suspension

Chemical compounds studied in this article

1-Ethyl-3-methylimidazolium acetate (PubChem CID: 11658353);

1. Introduction

Ionic liquids (ILs), a class of low-melting-point organic salts, are promising candidates as high performance "green" lubricants due to their negligibly low vapour pressure, excellent thermal stability, electrical conductivity and controllable physical and chemical properties. ILs are thus proposed to solve some of the most difficult lubrication problems occurring in a number of engineering applications (Palacio & Bhushan, 2010). For example, micro electrical mechanical systems (MEMS) require low-viscosity lubricants to overcome high static friction, while a number of medical- and bio-engineering applications require use of low vapour pressure lubricants with high electrical conductivity and heat capacity (Nainaparampil, Eapen, Sanders & Voevodin, 2007; Palacio & Bhushan, 2008; Pu, Jiang, Mo, Wang & Xue, 2011).

It was hypothesised that ILs may be effective lubricants due to formation of molecularly ordered layers at a static IL/solid interface that in turn would facilitate formation of a low-friction boundary when surfaces are set in relative motion (Horn, Evans & Ninham, 1988). However, experimental results demonstrated that these ordered layers can be disrupted in a rubbing contact, which results in the disappearance of an effective slip plane (Atkin & Warr, 2007) (Gebbie, Valtiner, Banquy, Fox, Henderson & Israelachvili, 2013; Min, Akbulut, Sangoro, Kremer, Prud'homme & Israelachvili, 2009; Perkin, 2012; Perkin, Albrecht & Klein, 2010; Smith et al., 2012). This complication can potentially be overcome through the use of additives. In particular, polymer additives are commonly used to enhance lubrication of aqueous and oil based lubricants to yield superior thin film and boundary lubrication properties. For ILs it was shown that the presence of adsorbed polymer layers that are also highly solvated can protect molecularly layered ionic structures from immediate destruction by shear forces, thereby preserving the low friction slip plane (Perkin, Albrecht & Klein, 2010). In

addition, in comparison to solvents alone, the presence of adsorbed polymers with high viscoelasticity have significantly better load bearing capacity, i.e., they cannot be easily squeezed out under compression (Harvey, Yakubov, Stokes & Klein, 2011).

Polysaccharide polymers, such as pectins, starches, chitosan, and cellulose are promising additives due to their low cost and abundance, and because they are highly soluble in ILs, which is a key pre-requisite for the formation of a solvated polymer film (Liu & Budtova, 2012). As it was recently shown, IL salts solvate polysaccharides by forming hydrogen bonds with their hydroxyl groups (Mateyawa et al., 2013; Remsing, Swatloski, Rogers & Moyna, 2006; Zhang, Liu, Xiang, Kang, Liu & Huang, 2014). These interactions disrupt the complex intermolecular hydrogen bonding network present in many polysaccharides and promote their dissolution. For examples, an IL, 1-ethyl-3-methylimidazolium acetate (EMIMAc) is used to solubilise waxy starches (Liu & Budtova, 2013), with the suggested conformation of amylopectin in EMIMAc being similar to the one observed in water, i.e., as a compact ellipsoid. It was also found that the mixed solvents of EMIMAc and water contribute to the complex phase transition in starches that involves gelatinization and dissolution, whereby two processes can occur either competitively or synergistically depending on the EMIMAc/water ratio (Mateyawa et al., 2013; Xie et al., 2014; Zhang et al., 2015).

Despite a promising set of properties, such as solvation, the mechanism of polysaccharide lubrication in ionic liquids remains totally unexplored. Furthermore, there is a degree of uncertainty whether addition of polymers will result in significant modification of boundary lubrication properties. In the boundary regime, the lubrication is dominated by the presence of an adsorbed film, the formation of which may be energetically unfavourable due to strong hydrogen bonding between IL and polymer molecules.

In this work, we show for the first time the enhanced lubrication of an IL-based solvent, which is achieved by using starch polysaccharides as an additive (0.1-0.5 wt%). Starch, as a biopolymer from agro-sources, has already attracted intense interest in materials science, especially for developing biodegradable plastics (Shogren, Fanta & Doane, 1993). Naturally in plants, it exists in the form of granules 1 μm – 100 μm in size; each granule is composed of alternating amorphous and semi-crystalline layers (growth rings) (100 – 400 nm in thickness); with the semi-crystalline layer in turn being formed by stacking crystalline and amorphous lamellae with periodicity of 9 – 10 nm. Starch consists of two major carbohydrates: amylose (mainly linear) and amylopectin (hyper-branched) (Fu, Wang, Li, Wei & Adhikari, 2011; Jane, 2009; Pérez, Baldwin & Gallant, 2009; Pérez & Bertoft, 2010). The structure of the granules varies significantly depending on the amylose/amylopectin content. For example, the granules of high-amylose starches are more compact with fewer voids, which makes them less accessible for solvents compared to low-amylose starches (Chen, Yu, Simon, Petinakis, Dean & Chen, 2009; Chen, Yu, Simon, Liu, Dean & Chen, 2011).

In the current work, we discover that the starch polymers leach into EMIMAc-water mixtures from starch granules at room temperature. The leached polymer is capable of reducing boundary friction

between rough polydimethylsiloxane (PDMS) elastomer substrates by up to 2.5 times compared to the pure solvent and up to 3 times compared to water. We also show that the presence of such soluble polymers results in the facilitation of suspension lubrication thereby enabling the use of starch suspension as lubricants without the need of separating insoluble materials.

2. Materials and methods

2.1. Materials, solution and suspension preparations

Two varieties of commercially available maize starches are used in this work, including waxy maize starch (Mazaca 3401X) (WMS), and Gelose 50 (G50); WMS is supplied by New Zealand Starch Ltd. (Onehunga, Auckland, New Zealand), and G50 by Ingredion ANZ Pty Ltd. (LaneCove, NSW, Australia). Both starches are chemically unmodified and the amylose contents for these two types of starches are 3.4 wt% and 56.3 wt% respectively, as measured by Tan et al. (2007)(Tan, Flanagan, Halley, Whittaker & Gidley, 2007) using the iodine colorimetric method. The original moisture contents are 12.4% and 13.6% respectively.

1-Ethyl-3-methylimidazolium acetate (EMIMAc) of purity ≥90%, produced by BASF, is supplied by Sigma–Aldrich, and is used as received without further purification. Deionized water is used in all instances.

EMIMAc-water mixtures are prepared by adding water to obtain desired EMIMAc/water mass ratios of 50/50, 55/45, 60/40, 65/35, and 70/30. Solutions are then placed on ice to minimise heating upon mixing. After 10-15 min, the solutions are placed in the fume hood at room temperature (24°C) to equilibrate for ~1h.

2.2. Starch suspension and solution preparations

Suspensions are prepared by mass by mixing an aliquot of starch into a measured amount of the EMIMAc-water mixture at room temperature (24°C). The suspensions are shaken for 1 minute and then stored for 24 hours prior to use.

Solutions of soluble starch are prepared by centrifugation of the suspension (4000g, 30 min) and separating the supernatant. Thereafter, an aliquot of the supernatant is precipitated with ethanol $(v:v=1:5)$. The precipitate is separated, dried (110°C, 12 h), and weighed. The solute content in the supernatant is then back calculated based on the mass of the precipitate. EMIMAc-water solvent is then used to adjust the concentration to the desired value. The precipitated material is also used for size exclusion chromatography (SEC).

The precipitate can be easily re-dissolved in the EMIMAc-water solvent, and the properties of the obtained solutions are identical to that of a supernatant. For simplicity, the supernatant solutions are used in a majority of the experiments.

2.2. Tribological measurements

The friction measurements are performed using a Mini Traction Machine (MTM, PCS Instruments Ltd, UK). The rubbing contact consists of a polydimethylsiloxane (PDMS) (SYLGARD® 184 Silicon Elastomer Kit, Dow Corning, MI) ball of radius 0.95 cm and PDMS disc of radius 23 mm and thickness 4 mm. The discs used are with two surface roughness values: 'smooth' with a root-mean-square (RMS) roughness of 9 nm, and 'rough' with an RMS roughness of 380 nm. The PDMS ball has only one surface RMS roughness at 26 nm. The Young's modulus of the PDMS is 2.4 MPa (Bongaerts, Fourtouni & Stokes, 2007). Untreated hydrophobic PDMS surfaces, water contact angle ca. 95°, were used unless stated otherwise.

In a typical MTM experiment, the ball and disc are driven independently at velocities v_b and v_d respectively, yielding the entrainment speed $U=(v_b+v_d)/2$. The relative motion of the moving ball and disc determine the slide-to-roll ratio, $SRR=(v_b-v_d)/U$. The lateral friction force F_i experienced by the ball is measured using a force transducer. To prevent offset errors, lateral force measurements are taken at each entrainment speed when $v_b > v_d$ and $v_b < v_d$, both rotating in the same direction, and the average was taken. Further details of the soft contact friction experiments are also presented elsewhere (Bongaerts, Fourtouni & Stokes, 2007). A load, *L*, is applied onto the ball and the normal force is measured using a strain gauge installed on the leaf spring of the MTM. The lateral friction force, F_f, and the normal load yield the friction coefficient, $\mu = F_f / L$. One way of representing friction in different lubrication regimes is using a so-called Stribeck curve, in which the friction coefficient is plotted against the product of U and the viscosity η. For each entrainment speed, at a constant SRR, ten friction measurements are taken and averaged. To test for hysteresis, each entrainment speed is tested twice in the same experiment; measurements are first taken from the highest speed 1000 mm/s and the speed is step-wise decreased to the lowest speed of 1 mm/s, after which the speed is increased again to 1000 mm/s.

For comparative purposes, to show how the starch alters the friction coefficient at a specific entrainment speed, a relative friction coefficient (μ_r) is used that is defined as the ratio of the friction coefficient for a starch solution in EMIMAc-water and a reference solution. The reference solution is either water or the solvent in which the starch is dispersed:

$$\mu_r = \frac{\mu_{solution}}{\mu_{reference}}$$

2.3. Dissolution, debranching, and analysis of starch molecules using size-exclusion chromatography (SEC)

In order to analyse composition of the dissolved starch , the precipitated material (see section 2.2 for details) (~6 mg, dry weight) is dissolved in 1 mL dimethylsulfoxide (DMSO; GR for analysis ACS, Merck & Co, Inc., Kilsyth, VIC, Australia) containing 0.5 wt % LiBr (ReagentPlus, Sigma–Aldrich, Castle

Hill, NSW, Australia) (DMSO/LiBr solution) using a thermomixer (Eppendorf, Hamburg, Germany) at 80°C and 350 rpm for 12 h and then debranched using isoamylase from *Pseudomonas* sp. (Megazyme International, Bray, Co. Wicklow, Ireland) in acetate buffer (pH ~3.5), following the method of Li et al. (2014) The weight distributions of the whole (fully branched) and debranched starch molecules is analysed in duplicate using SEC (Agilent 1100 series, Agilent Technologies, Waldbronn, Germany) equipped with a refractive index detector (Shimadzu RID-10A, Shimadzu Corp., Japan). SEC separates molecules based on their hydrodynamic volume (V_h), or the corresponding hydrodynamic radius (R_h). Following the method of Cave et al. (2009), pullulan standards with peak molecular weights ranging from 342 to 2.35×10^6 were used to obtain the universal calibration to convert the elution volume to the hydrodynamic volume (V_h), and the corresponding hydrodynamic radius (R_h), whereby $V_h = 4/3 \pi R_h^3$.

2.4. Rheological measurements

Rheological measurements are carried out at 24°C on a TA AR G2 (New Castle, Delaware, USA, TA Instruments) rheometer using a 40 mm Titanium parallel-plate in combination with the manufacturer's Peltier Plate unit; a cover is placed over the geometry and small drops of solution are placed around the perimeter of the sample (but not touching the sample) to limit evaporation/water absorption. To obtain reliable viscosity data on the diluted samples, the narrow gap approach is used (as reported elsewhere (Boehm, Shewan, Steen & Stokes, 2015; Davies & Stokes, 2008; Stokes, Davies, Macakova, Yakubov, Bongaerts & Rossetti, 2008)). Briefly, gaps on the order of 10 µm are used to achieve shear rates on the order of 10^5 s^{-1}, which places measurements in an accessible torque range; one must be certain, however, that the Reynolds number is less than 100, otherwise inertial forces contribute. The narrow gap approach is made possible by, first, determining the gap error then adjusting the experimental data according to well-documented mathematical procedures (Davies & Stokes, 2005; Kravchuk & Stokes, 2013). Additionally, samples are precision loaded via micropipette (Transferpette 10 µL-100 µL, BrandTech). The exact volume is calculated based on the diameter of the geometry and the gap plus the gap error, with an additional ≈ 0.5 µL to provide a slight overfill that can be trimmed.

2.5. Ellipsometric measurements

Thickness measurements of an adsorbed layer of starch on a model hydrophobic surface are performed using a J. A. Woollam vertical variable angle spectroscopic ellipsometer V-VASE (USA) equipped with a 5 mL vertical liquid cell (model TLC-100). The model surface is a mixed alkanethiol layer on gold (Sedeva, Fornasiero, Ralston & Beattie, 2010), formed by adsorption from an ethanol solution consisting of 0.3 mole fraction of 16-mercapto-1-hexadecanol ($HO\text{-}(CH_2)_{16}SH$, 99%, Frontier Scientific) and 0.7 mole fraction of 1-hexadecanethiol ($CH_3(CH_2)_{15}SH$, 95%, Sigma Aldrich), of total thiol concentration 10 mM. The gold substrate is produced by CVD, as described and characterised elsewhere (Beattie et al., 2015). The thiol-coated substrate has an advancing water contact angle ~90°, making the surface of similar hydrophobicity to PDMS, and thus a viable substrate for starch adsorption.

For all measurements, the ellipsometric parameters, Ψ and Δ (amplitude ratio and phase difference of reflected p (r_p) and s (r_s) polarized light), are measured for the required range of wavelengths (400-1000 nm) at the angle of incidence close to 75°:

$$\tan(\Psi)\exp(i\Delta) = \rho = \frac{r_p}{r_s}$$

These data are acquired for the underlying gold substrate without any liquid present, and for the EMIMAc-water solvent above the silicon wafer calibration standard for the liquid cell. These measurements are used to generate optical constants for the substrate and the solvent (using the WVASE32 software from JA Woollam, USA), which are then used to enable data from the adsorption experiment to be analysed, using a three layer model (thiol-coated gold/starch adsorbed layer/EMIMAc-water ambient solution). The thickness of the starch layer was obtained by fitting the polymer layer as a single Cauchy medium (Born & Wolf, 1999) (which assumed the layer is homogeneous and transparent). In order to determine thickness, the refractive index of the adsorbed layer at 590 nm was taken to be 1.48. This value is realistic when one considers the refractive index of non-hydrated starch granules (1.50) (Luallen, 2002) and the refractive index of the solvent (1.45).

2.6. Optical microscopy

Optical characterisation of the starch suspension is performed using a LSM 100 (Zeiss, Germany) inverted optical microscope for differential interference contrast (DIC) imaging and an upright AxioScope A1 (Zeiss, Germany) microscope for polarised light imaging. A small drop of starch suspension (with 0.5 wt% starch content) is transferred by a micro-pipette onto a glass slide which is then covered by a 0.17 mm glass cover slip. A range of magnifications from ×100 to ×630 is used. All microscopy experiments are done at room temperature. Acrylate solution was used to seal the sample between two glass surfaces to avoid evaporation during observation.

3. Results and Discussion

3.1. The effect of EMIMAc-water mixture composition on the starch granule morphology and leaching of starch material.

The G50 suspended in EMIMAc-water mixture shows a partial leaching of starch material from the granules into the soluble phase. As a result, a molecular solution of amylose and amylopectin forms. The solubility of the G50 starch in the EMIMAc-water mixtures displays a transition for EMIMAc concentration between 55 and 60 wt%. For EMIMAc/water composition at and above 60/40 (i.e., EMIMAc/water solvent weight ratio), the solubility is found to increase ~100 times, as shown in Figure 1. The character of this transition and the concentration of the solvent mixture are similar to

the plasticising transition of the starch granules observed previously (Mateyawa et al., 2013). The morphology of starch granules (Figure 2) and their birefringence (Figure 1, Supplementary Information) - which is a useful proxy for starch crystallinity - was also found to change with the change in EMIMAc-water composition. In 50/50 solvent mixture, the structure of the granule changes little compared to water alone. However at 55/45, changes in morphology and birefringence can already be observed. For 60/40 solvent mixtures, a clear change in morphology (i.e., loss of clear granule boundaries and an increase in the apparent granule size) is accompanied by some loss of birefringence. For the 65/35 solvent mixture, birefringence reduces further and morphological changes occur with the appearance of a characteristic roughness and pitted morphology of starch granules (Figure 2, Supplementary Information). With further increase in EMIMAc content, i.e., 70/30 solvent mixture, the swelling of starch granules becomes more apparent to such a degree that through centrifugation one can isolate a partially gelatinised fraction of granules with lower density, which appears as a translucent layer of annealed granules sitting on top of the more dense and opaque layer of compacted granules (Figure 3, Supplementary Information). The swelling of the particles results in their size increasing by ~30% in 70/30 solvent mixture compared to water.

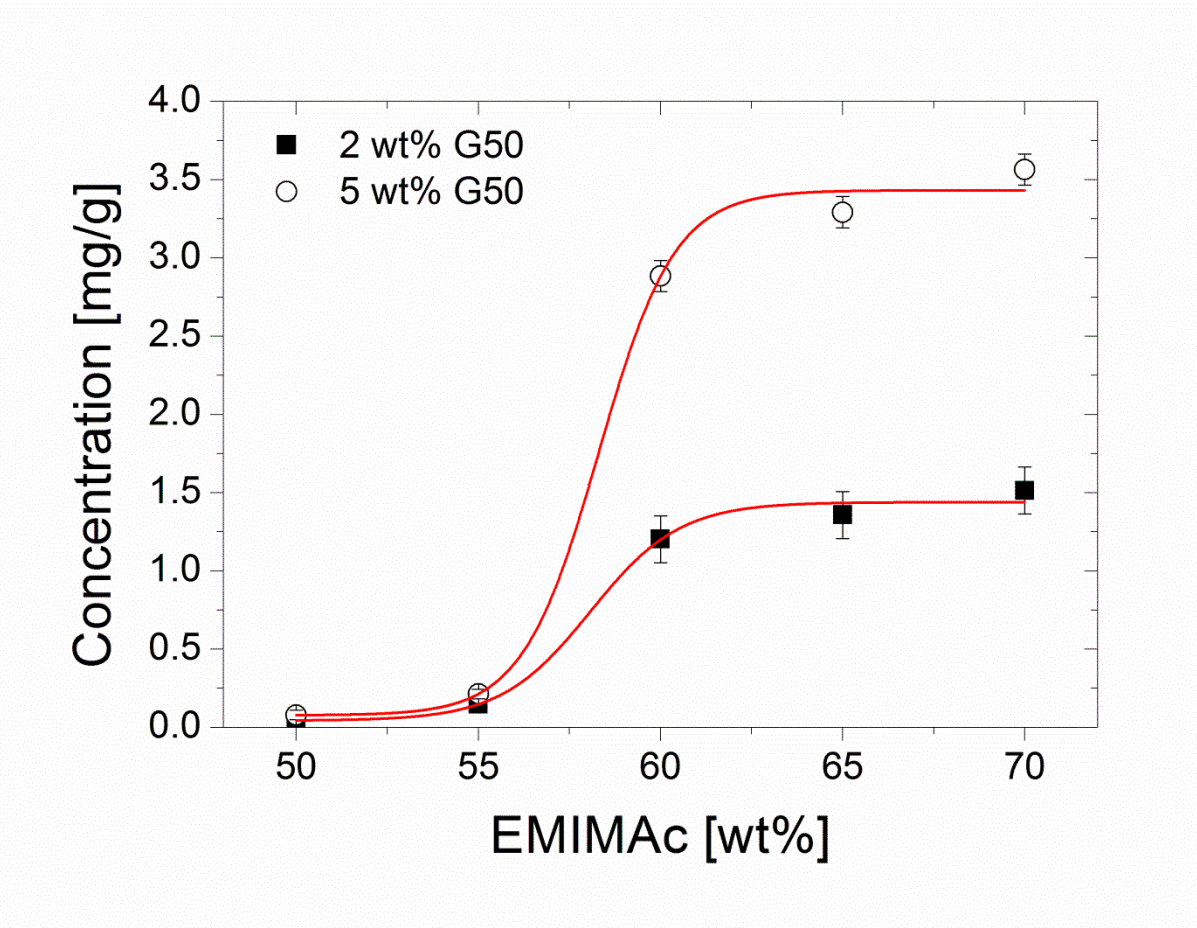

Figure 1. Characterisation of solubility of G50 starch in EMIMAc/water mixtures. The graph plots the solubility of G50 starch as a function of solvent composition for the 2 wt% and 5 wt% G50

suspensions. The red lines are Boltzmann sigmoidal function fitted to the data.

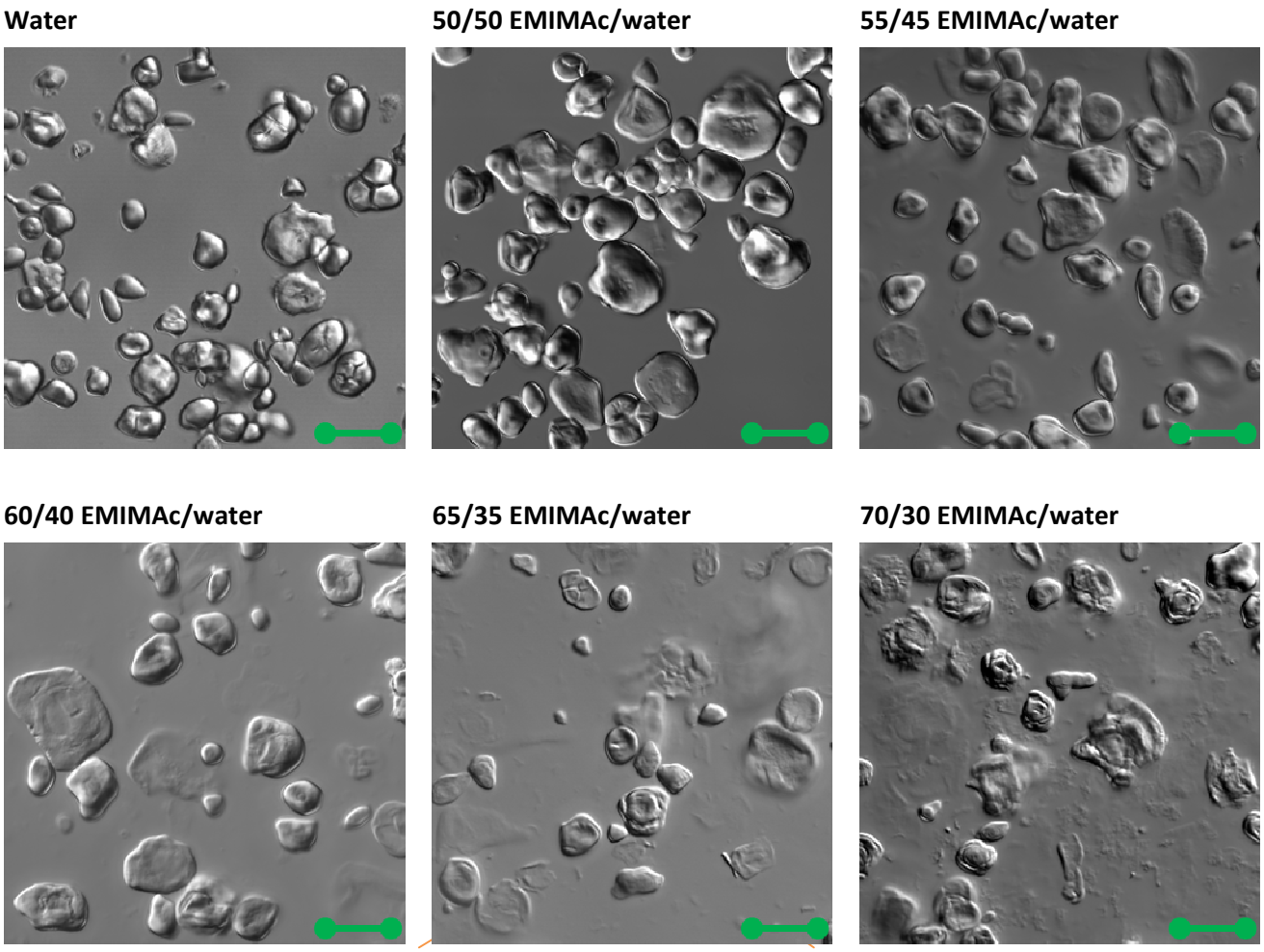

Figure 2. Differential interference contrast (DIC) microscopic images of G50 starch in different EMIMAc-water solvents. The use of DIC microscopy enables to highlight the changes in the surface structure of the granules that undergo leaching of the material into the solvent. Scale bar is 20 µm.

The dependency of the solubility on the concentration of starch granules (Figure 3A) was found to be linear with the starch granule mass concentration. Such dependency indicates that within a starch granule only a small fraction of the starch leaches into solution while the bulk of starch material remains undissolved. The increase in temperature (Figure 3B) results in the increase in the amount of the leached material, as expected. The result suggests that upon temperature induced swelling of starch granules more areas of starch granule become available and the EMIMAc-soluble starch

fraction may be liberated from the inner parts of the granule, as opposed to predominately surface leaching observed at lower temperatures. The dependency of solubility on temperature is found to be linear, which supports the hypothesis that the leaching is associated with the release of a specific fraction of starch. If alternative scenarios would be at play, the solubility would follow Arrhenius-like behaviour.

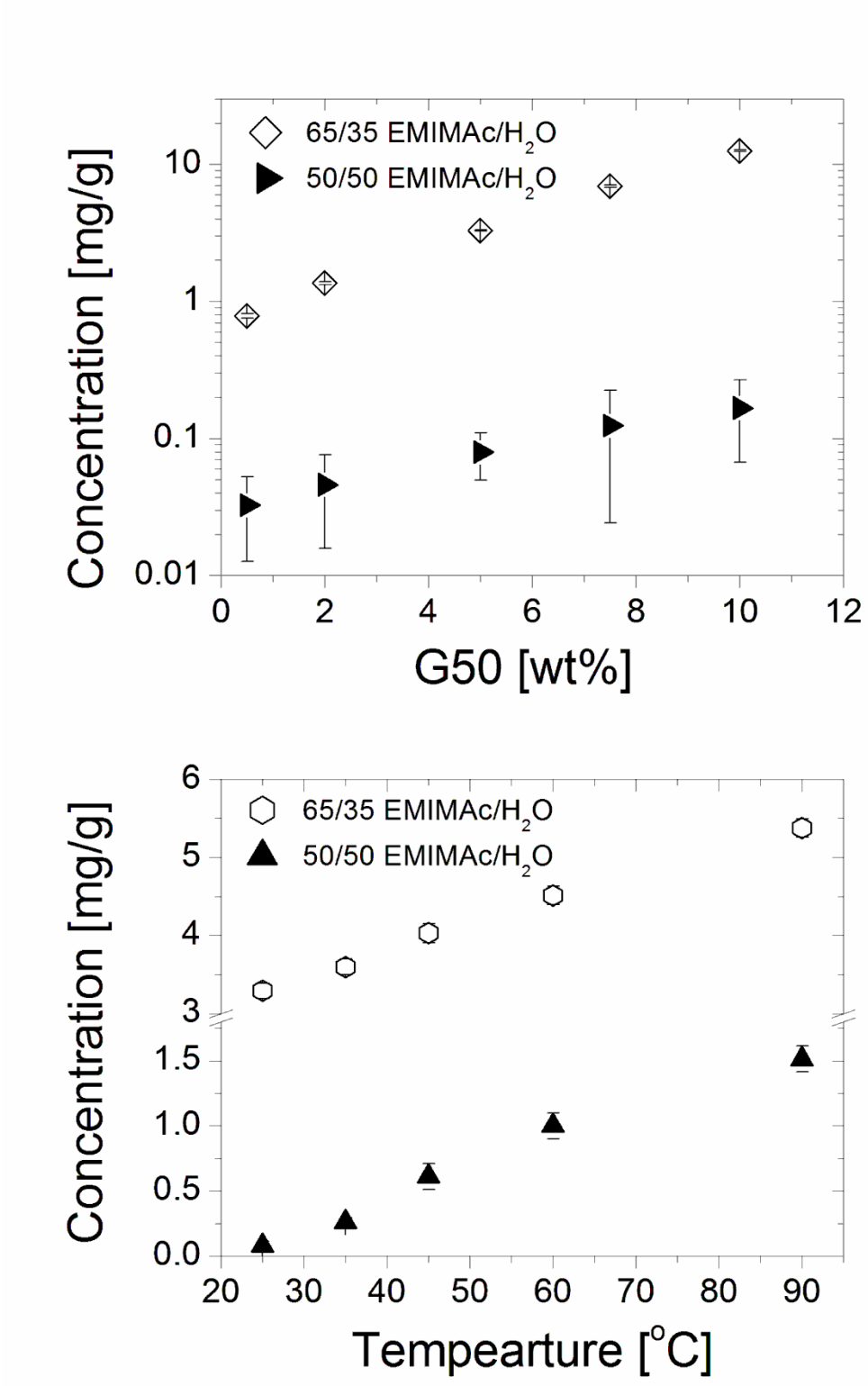

Figure 3. Characterisation of solubility of G50 starch in EMIMAc/water mixtures. Panel (A) plots the solubility of G50 starch as a function of suspension concentration for two solvent compositions sitting below and above solubility transition. Panel (B) plots the solubility of G50 starch as a function of temperature for two solvent compositions sitting below and above solubility transition.

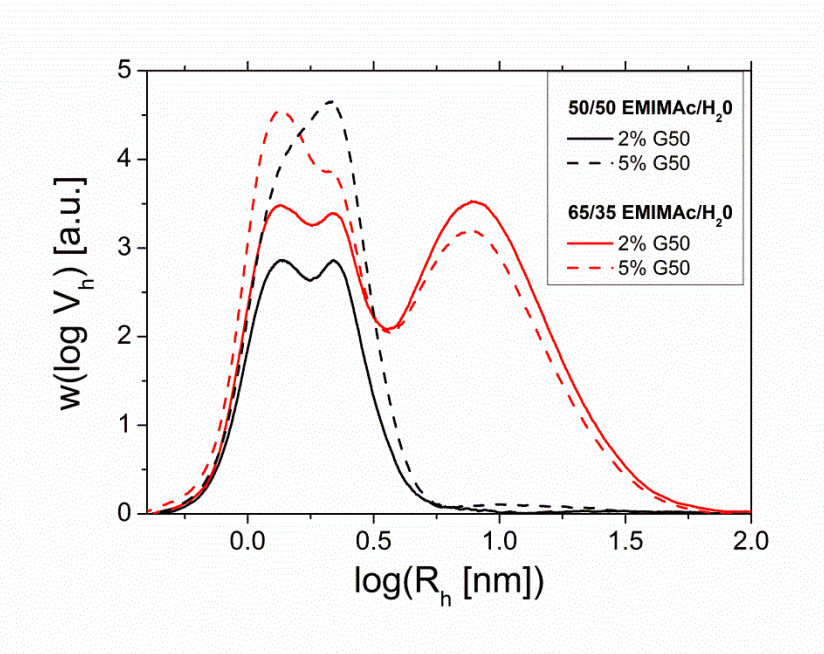

Sample	Amylose%
50/50_2%	1.3%
50/50_5%	2.5%
65/35_2%	55.1%
65/35_5%	46.9%

Figure 4. Size distribution of the debranched IL-soluble starch. Chromatograms are recorded for two EMIMAc/water ratios; 50/50 (black lines) and 65/35 (red lines). The extraction of starch was performed from 2% (solid lines) and 5% (dashed lines) G50 suspensions. The table in the inset shows the weight % of amylose in the extractable sample.

The nature of the molecular species partitioned into the liquid phase was found to be similar to that of native starch, i.e., amylose and amylopectin. The size exclusion chromatography of hydrolysed samples showed a dramatic change in the composition of the soluble starch depending on the composition of solvent (Figure 4). For solvents containing < 60 wt% EMIMAc, the predominant molecule leached from the granules is amylopectin (>90 wt% of the total soluble starch), with amylose accounting only for ~1-2 wt%. For solvents containing ≥ 60 wt% EMIMAc, which is above the solubility transition, the fractions of amylose and amylopectin leached into the solvent are roughly equal; this ratio roughly corresponds to the composition of G50 starch, which has an amylose content of 56.3 wt%. Although the reason behind the difference in the solubility of amylose and amylopectin in EMIMAc-water mixtures < 60 wt% is unclear, it is possible to suggest that for low levels of solubility the heterogeneity of starch granule structure and composition may affect the result (Dhital, Shelat, Shrestha & Gidley, 2013).

The analysis of molecular weight under native conditions (i.e., without hydrolysis) showed a slight decrease in the amylose molecular weight compared to native starch, however the decrease is found to be marginal (Figure 4, Supplementary Information). Both chromatography results were similar for materials isolated from 2 wt% and 5 wt% suspension, suggesting that solutions formed under both conditions are below the solubility limit of amylose and amylopectin in the respective solvents.

3.2. Boundary lubrication of Solubilised Starch between Hydrophobic surfaces

For the lubrication study, we utilise the G50 starch polymers extracted from dissolution in 65/35 solvent mixture where there is equal proportion of dissolved amylose and amylopectin. Lubricants are produced by adding either water or EMIMAc to the 65/35 supernatant (after centrifugation) that contains the solubilised species to investigate how they affect lubrication under different solution environments (solvent ratio), which is expected to influence the conformation of the polymers and their adsorption to PDMS surfaces. In addition, the 65/35 solvent mixture is also used to extract leachable material from waxy maize starch (WMS), which contains predominantly amylopectin. From this preparation, 0.25 and 0.33 wt% starch solutions are prepared. WMS showed high solubility in 65/35 and desired concentrations were achieved using only 0.5 wt% of WMS suspension.

To detect and confirm the presence of an adsorbed layer of starch, ellipsometry measurements are performed on a model hydrophobic surface (alkanethiol on gold) of similar hydrophobicity to PDMS using 0.31 wt% solution of the G50 starch soluble polymer in the 65/35 solvent. First, the pure 65/35 solvent was passed over the substrate, followed by injection of the starch solution and an adsorption equilibration period of 20 minutes. Prior to evaluating ellipsometric parameters, Ψ and Δ, the fluid cell was flushed with pure solvent, thus leaving behind only strongly adsorbed polymer. The fit of Ψ and Δ plots versus incident wavelength (Figure 5, Supplementary Information) yielded an effective thickness of the polymer layer of 20.3 ± 2.1 Å.

The lubrication in our soft-tribological contact by EMIMAc-soluble starch components depends on both the solution environment (EMIMAc/water mixture ratio) and starch concentration. In Figure 5A, μ_r at 5 mm/s is shown for 0.25 wt% soluble G50 starch solutions within different EMIMAc/water solvents, and for the solvent relative to water. The results are summarised in Table 1. The μ_r for the solvent decreases with increasing EMIMAc content. Of the solvent mixtures, the 70/30 solvent mixture has the lowest μ_r; this is due to it having a significantly higher viscosity than the other solvents such that viscous forces contribute to the frictional response and the system is in the mixed lubrication regime. The soluble G50 starch results in a significant decrease in friction coefficient compared to their respective solvents; for all starch solutions except 70/30 solvent mixture, $\mu_r \sim 0.5$. For the 70/30 solvent mixture, higher values of μ_r are observed which is likely due the polymers having less effect in the mixed boundary regime where the viscosity of the solvent contributes significantly to the friction.

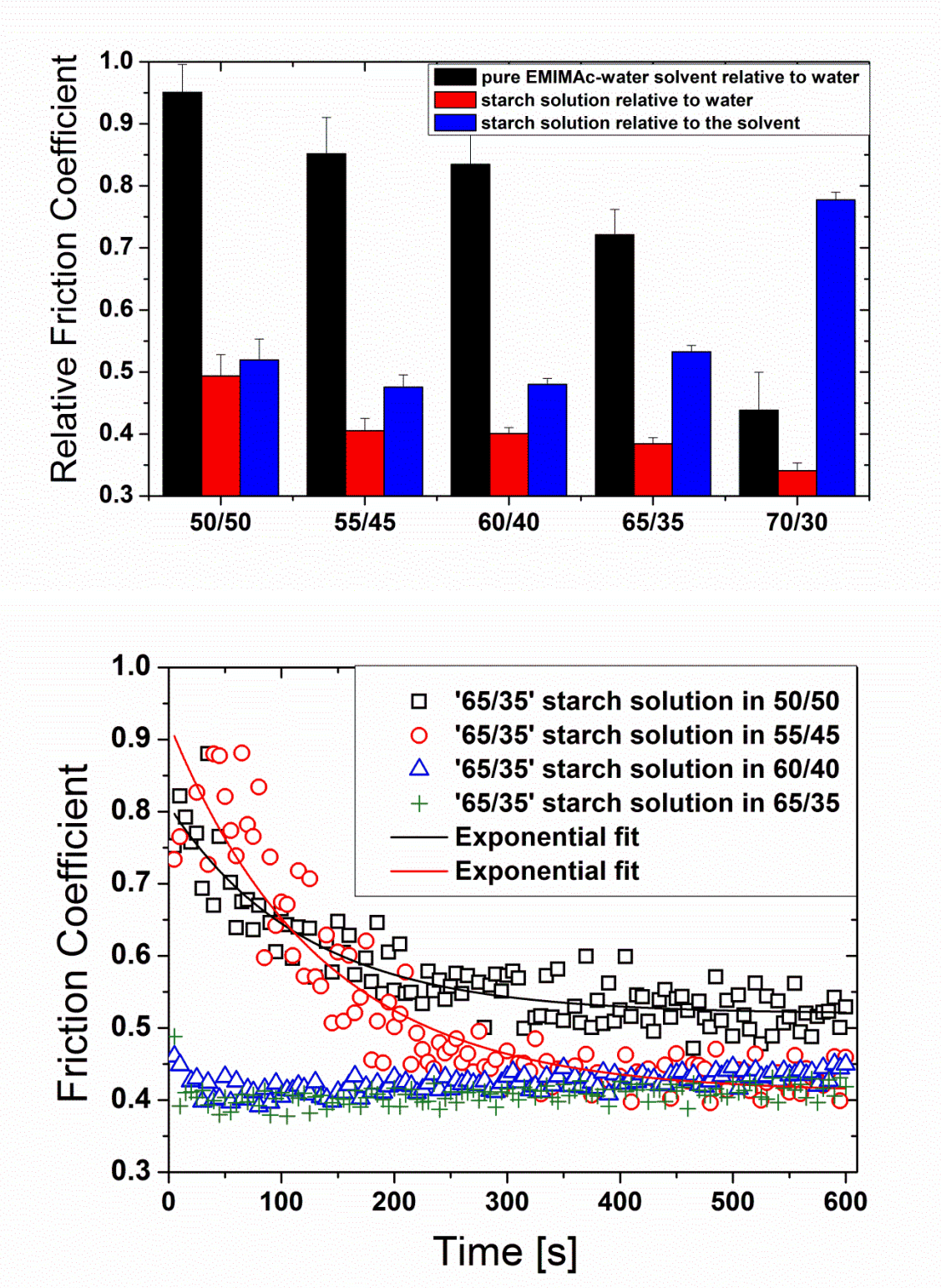

The friction results given in Table 1 demonstrate that the G50 starch polymers (in 65/35 solvent mixture) are more effective boundary lubricants than WMS starch polymers. These two starch types

differ in terms of the main polymers extracted from the starches in the EMIMAc/water solvent; amylose and amylopectin is mainly solubilised from G50 starch; while amylopectin is the main polymer extracted from WMS starch. It is therefore suggested that the amylose leached from G50 is more active as a boundary lubricant than amylopectin. We note that the leachable starch material comprises only a very small fraction of the total starch, and since the SEC results showed a detectable decrease in molecular weight of leachable amylose compared to native starch, it is possible to suggest that the solubility of amylose is highly selective in EMIMAc/water mixtures, and potentially depends on the structure of amylose inside the granule and its molecular weight.

Despite the fact that the boundary friction coefficient for G50 starch in 50/50, 55/45, and 60/40 solvent mixtures are very similar, the evolution of friction force with time of measurement displays dramatic difference as shown in Figure 5B. For the G50 starch solutions in 50/50 and 55/45 solvent, we observe a slow decrease in friction that roughly follows the exponential decay $\left(\mu \propto e^{-t/\tau}\right)$ with the characteristic time decay, τ, of 120-130 s^{-1}. In contrast, a steady state is achieved almost immediately after the lubricant is deposited on the PDMS surface for the G50 starch in 60/40 and 65/35 solvent mixtures. We suggest that the results indicate that as the amount of EMIMAc is decreased from the original 65/35 EMIMAc/water mixture, the solution environment is less favourable and the conformation of starch polymers is altered from being expanded and highly soluble to one that is a more collapsed and less soluble.

To investigate further the effect of solvent changes on friction of solubilised starch polymers, we compare μ_r in various solvents after extraction of soluble polymers from G50 starch into 50/50 (less soluble, 0.008%) and the 65/35 (more soluble, 0.23%) mixture solvent. The tribology experiment is performed by forming lubricating films with these extracted solutions, measuring the friction coefficient at 5 mm/s until steady state is reached, and then adjusting (exchanging) the background solvent in the tribometer to either 65/35 and 50/50 EMIMAc/water ratios respectively.

The steady state μ_r values for the G50 starch solutions, relative to water and solvent, are given in Table 2. In regards to the G50 starch extracted into 50/50 solvent mixture, there is a 20% decrease in friction coefficient due to the presence of starch ($\mu_r \sim 0.8$), and this is unaffected by improving solvent quality by exchanging it to the 65/35 solvent mixture. In contrast, there is a 50% decrease in friction from the presence of G50 starch extracted into 65/35 solvent mixture, i.e., $\mu_r \sim 0.5$ (relative to solvent). When the 65/35 solvent is changed to the 50/50 mixture, which is of lower solvent quality and thus a less favourable environment for the starch polymers, the friction increases dramatically. We note that after the solvent exchange to the 50/50 mixture the friction for '65/35' extractable material is similar to that found for the '50/50' material, despite a large difference in starch concentration; 0.23% versus 0.008% correspondingly.

The result of this experiment strongly suggests that the lubrication properties of the surface film are sensitive to solvent quality. When the starch polymers are adsorbed in favourable environment, a subsequent decrease in solvent quality (as indicated by decreased solubility) causes the responsive adsorbed polymer films to become more compacted and less-solvated, which is less lubricating (higher boundary friction). Such a link between solvation and lubrication of polymeric surface films has been documented in numerous aqueous systems such as molecular brushes and proteinaceous layers (Klein, Zhang & Wilhelm, 2000; Macakova, Yakubov, Plunkett & Stokes, 2010, 2011; Yakubov, Macakova, Wilson, Windust & Stokes).

3.3. Tribological behaviour of starch suspensions and the influence from solubilised starch polymers

Starch suspensions refer to the full suspension of starch in water or EMIMAc/Water mixtures prior to centrifugation; it therefore contains both soluble and insoluble species. The tribological behaviour of starch suspension is assessed using roughened PDMS surfaces; rough surfaces are employed to facilitate entrainment of insoluble particle as shown previously for glass spheres suspensions (Yakubov, Branfield, Bongaerts & Stokes, 2015) and hence probe more directly the effects associated with the friction between starch suspensions and the PDMS surfaced.

In Figure 6A, the Stribeck curves for water and G50 starch suspensions (0.5 wt% and 2 wt%) in deionised water are presented. Due to a combination of the compliant nature of the elastomer substrates and roughness, a characteristic decrease in friction coefficient with decreasing speed is observed even for a Newtonian fluid (water) (Persson, 2000). The presence of starch granules results in the decrease in the friction coefficient, with Stribeck curve for the suspension qualitatively following a Newtonian Stribeck curve down to $U\eta \sim 10$ μN/m. Below ~ 10 μN/m, the presence of the suspension results in further enhancement of lubrication compared to water, which appears on the graph as the widening of the gap between the Newtonian and suspension Stribeck curves. Such a decrease in friction at low speeds was observed and examined in detail previously using model suspensions of glass beads in various Newtonian solvents. Based on this parallel observation, we can hypothesise that the reduction in friction at low speeds ($U\eta < 10$ μN/m) is associated with the entrainment of particles into the contact and the subsequent change from sliding- to rolling-dominated friction, whereby entrained particles provide a ball-bearing effect (Yakubov, Branfield, Bongaerts & Stokes, 2015).

In Figure 6B, the Stribeck curve for G50 starch suspensions in water measured at 60°C illustrates the effect of the temperature when starch granules are more swollen compared to their state at room temperature. In this case, a significant change in the Newtonian master curve is associated with softening of the PDMS at elevated temperatures. The characteristic positive slope of the apparent boundary regime is again associated with the viscoelastic effects in the compliant substrate(Bongaerts, Fourtouni & Stokes, 2007; Persson & Scaraggi, 2009; Scaraggi & Persson, 2014). The G50 suspensions marginally reduce friction in a similar fashion to the case at the room temperature; however, it appears that the shape of the curve for the suspension is similar to the

Newtonian master curve, suggesting minimal contribution from the particle ball-bearing effect. This hypothesis is tested further by performing measurements at 60°C on the G50 suspension that prior to measurements has been gelatinised at 95°C for 4 hours (Figure 6C). Gelatinisation results in the deformation of starch granules, with many particles adopting irregular shapes, as can be seen in Figure 6D. The Stribeck behaviour of such irregularly shaped particles was found to be identical to non-gelatinised starch particles. This result enables us to conclude that the reduction in friction coefficient is not associated with the ball-bearing effect. Instead, the reduction in friction is likely to be associated with granules being trapped within surface asperities, which reduces the effective area of highly frictious PDMS-PDMS contact and provides enhancement of lubrication. It is also evident that at room temperature this entrapment effect dominates the Stribeck behaviour, with only a small contribution coming from particle ball bearing effect at low entrainment speeds. The reduction in friction also depends on the particles' phase volume, which is particularly evident from the Stribeck curves recorded at 60°C, which is associated with the increased probability of particle entrainment into the contact for more concentrated suspensions. At both temperatures we observed a hysteresis between the Stribeck curves recorded on the ascending and descending ramp of the speed, with the ascending curve usually positioned slightly higher than the descending one. The origin of hysteresis can be either associated with the accumulation of starch granules at the inlet of the rubbing contact (Gabriele, Spyropoulos & Norton, 2010), as well as with sedimentation of starch granules.

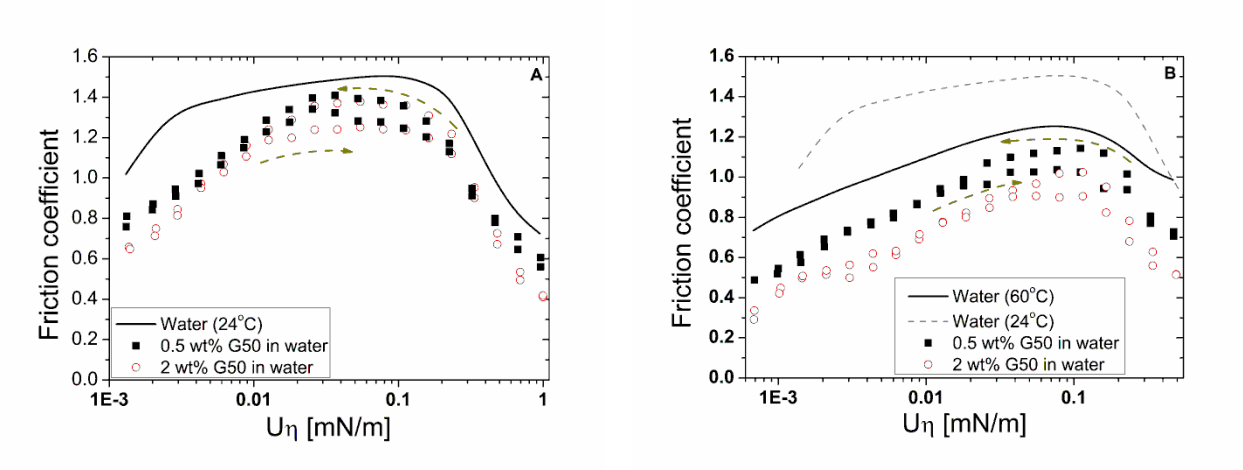

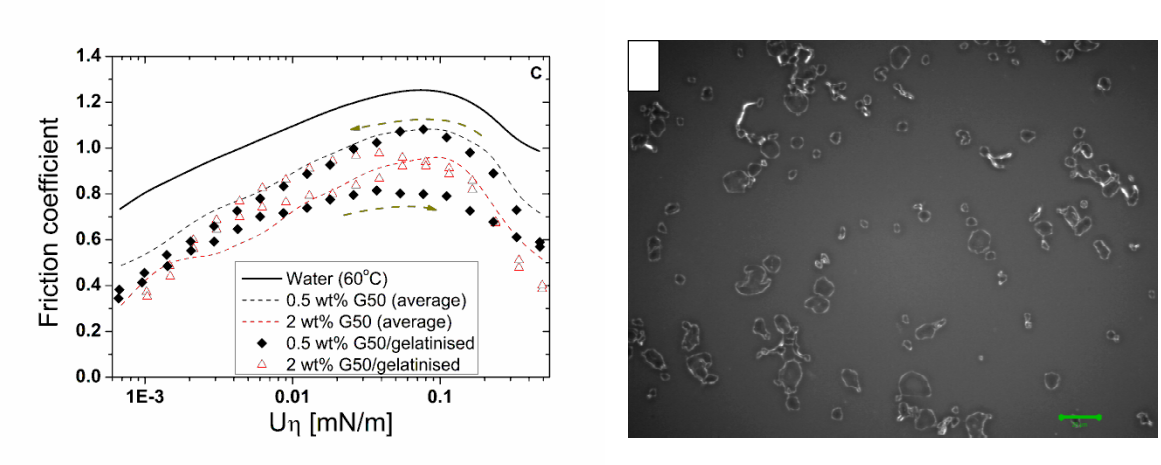

Figure 6. Stribeck curves for 0.5 and 2% G50 suspensions in water using rough surfaces. (A) 24°C; (B) 60 °C; and (C) 60°C gelatinised (at 95°C) suspensions. The Stribeck curves corresponding to pure water measured against the same substrate and temperature are displayed for reference. The dashed arrows indicate the direction of the speed ramp, and indicate the observed hysteresis. (D) A polarised light microscopy image of the gelatinised sample (0.5 wt% G50, scale bar 20μm).

The Stribeck behaviour of EMIMAc-water mixtures is shown in Figure 7. The EMIMAc-water solvents display a clear enhancement of lubrication in the mixed regime, while the facilitation of boundary lubrication compared to water is modest. This behaviour is consistent with our observation that EMIMAc-water mixtures have a lower contact angle on the hydrophobic PDMS compared to water, which facilitates fluid entrainment into the gap between surfaces. This in turn extends the range of the elastohydrodynamic lubrication to the lower values of Uη, which in turn shifts the onset of the mixed lubrication regime to lower Uη. The result also demonstrates that potential layering at the solid liquid interface for the EMIMAc-water solvents is not translated into the effective boundary lubrication effect, probably due to disruption of such layers under rubbing conditions (Atkin & Warr, 2007; Min, Akbulut, Sangoro, Kremer, Prud'homme & Israelachvili, 2009).

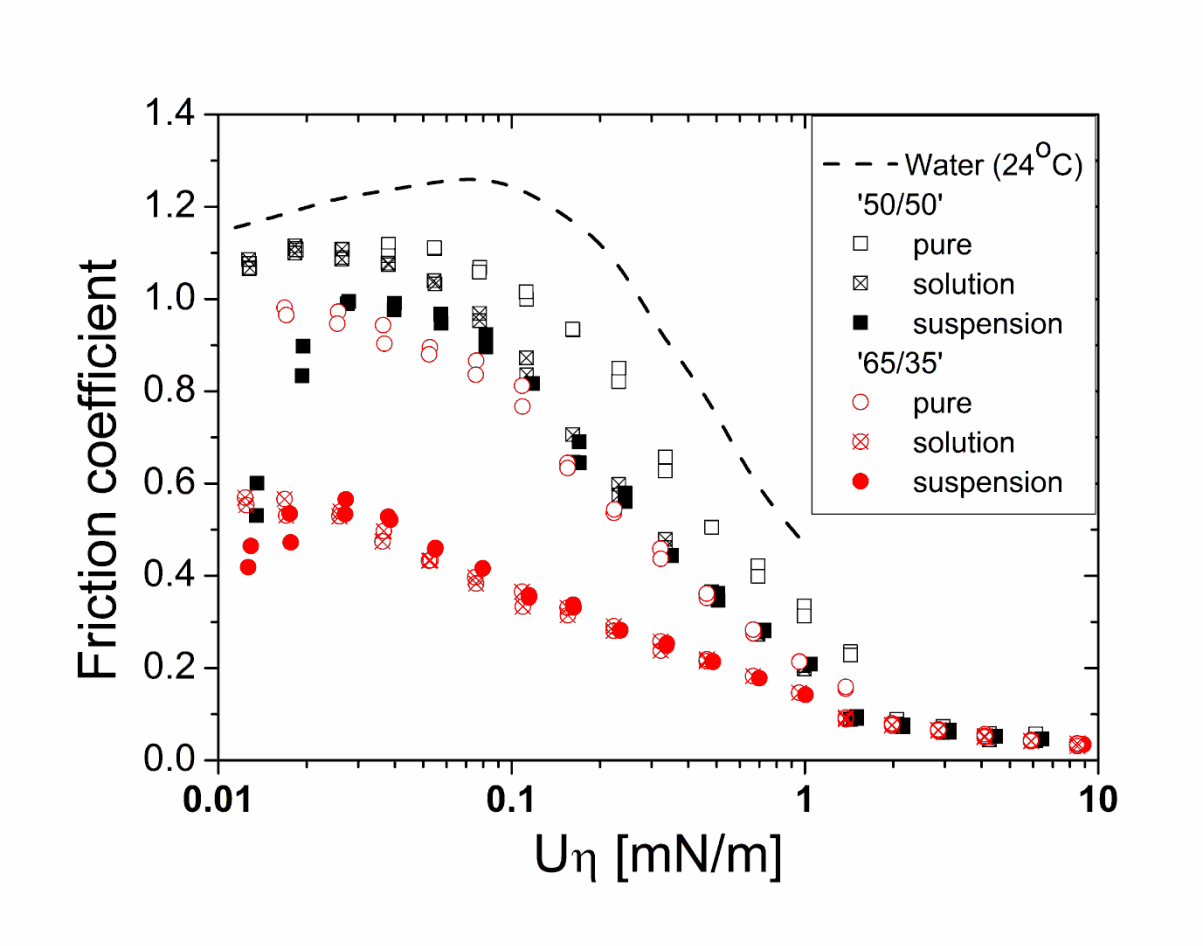

Figure 7. Stribeck curves for two representative EMIMAc-water solvents; '50/50' (squares) and '65/35' (circles). Open symbols correspond to pure solvent, crossed symbols to the solution of soluble starch fraction extracted from G50, and solid symbols are to the 2% G50 suspension. The Stribeck curves corresponding to pure water measured against the same substrate and temperature are displayed for reference. All measurements were done at 24°C.

The presence of soluble starch was found to significantly affect Stribeck behaviour. For the 50/50 solvent mixture, the presence of soluble starch results in the shift of the mixed regime to the low values of Uη, with boundary friction coefficient; however, remaining largely unaffected (see also Figure 5 for the reference). We note that both curves are normalised against their respective viscosities, and therefore the shift in the mixed regime is not associated with the bulk viscosity. We also note that the transition from the elastohydrodynamic regime to the mixed one occurs at the same value of Uη for both fluids. This suggests that potential difference in wettability and the resulting enhancement of fluid entrainment is unlikely to be a key driving mechanism. The observed behaviour, however, would be consistent with a scenario whereby the effective local viscosity of the fluid confined within the asperities increases with decreasing Uη. It is plausible to hypothesise that starch molecules soluble in the 50/50 solvent could form a weakly adsorbed/associated layer that changes the local viscosity of the fluid in the vicinity of the surface, leading to an apparent

enhancement of mixed lubrication. On the other hand, such a 'film' has not significantly enhanced lubrication in the boundary regime where surfaces are in more intimate contact.

By contrast, the behaviour of starch solutions in the 65/35 solvent mixture shows qualitative changes in both mixed and boundary regimes. The boundary friction, as discussed in the previous section, decreases by about 50%, while the mixed regime appears to have a much lower slope $\left(\frac{\partial \mu}{\partial U}\right)$ compared to the solvent. Even by shifting the Stribeck curves using a hypothetical value of effective viscosity one would not be able to match the solution with the solvent. Such behaviour confirms ellipsometry data and is suggestive of a stable boundary film that prevents direct PDMS-PDMS asperity contacts and facilitates fluid entrainment into the narrow gap.

As expected, the behaviour of 2% G50 starch suspensions largely follows that of the respective solutions, with deviations becoming apparent only at low $U\eta$. For the suspension in 50/50 solvent mixture, one can observe a clear decrease in the friction coefficient for $U\eta < 0.03$ mN/m, which is qualitatively similar to the behaviour of granules in water associated with the facilitation of lubrication via a particle ball-bearing mechanism. For the suspension in 65/35 solvent mixture, the deviation from the respective solution is minimal. This suggests that the boundary film formed by the soluble starch molecules inhibits the ball-bearing effect of the granules. Most likely, this is due to a significant reduction in the sliding friction between the granule and film-modified PDMS surface.

Figure 8 presents the results of the tests for a set of solvents (from 50/50 to 70/30 EMIMAc-water mixtures) that illustrates the dependency of the Stribeck behaviour of suspension on solvent, G50 starch concentration, and temperature. The changes in the Stribeck behaviour clearly follow the solubility of the starch in the EMIMAc-water solvent. At room temperature one can see that the biggest transition occurs between 55/45 and 60/40 solvents, which matches exactly the transition in the solubility and the change in composition of soluble starches. For concentrations above 60 wt% EMIMAc, Stribeck results display no further change.

With increasing suspension concentration from 0.5 wt% to 2 wt% G50 starch, a contribution from particle ball bearing becomes apparent, whereby 2% G50 starch suspensions display a stronger drop in friction coefficient at lower values of $U\eta$. This is associated with the increased probability of particle entrainment and confinement between PDMS surfaces. Although the behaviour of starch suspensions in 50/50 and 55/45 solvents are similar, there is a difference in the hysteresis between Stribeck curves recorded with increasing and decreasing speeds. This is indicative of a contribution from sedimentation whereby sedimentation is more pronounced in less viscous 50/50 solvent.

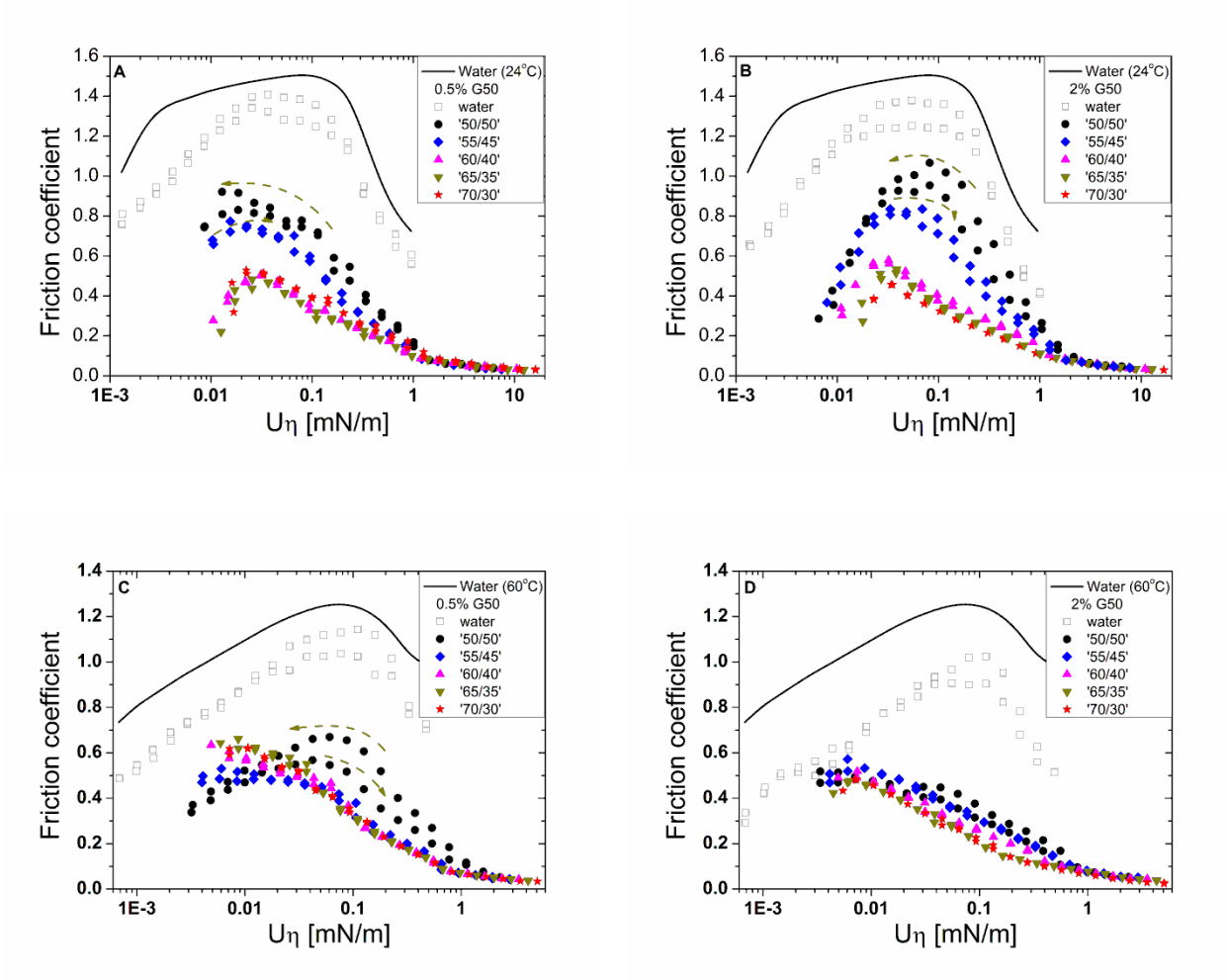

Figure 8. Stribeck curves of G50 suspensions in various solvents. (A) 0.5 wt% G50 at 24°C; (B) 2 wt% G50 at 24°C; (C) 0.5 wt% G50 at 60°C; (D) 2 wt% G50 at 60°C. Open symbols correspond to pure G50 suspension in pure water (see Figure 6 for more details). The Stribeck curves corresponding to pure water measured against the same substrate and temperature are displayed for reference.

This Stribeck behaviour changes when experiments are performed at 60°C. Under these conditions the 2 wt% G50 starch suspensions in all solvents behave nearly identical, which is likely to be associated with the increased concentration of the starch material in the solution (Figure 3B). It appears that for all solvents at 60°C enough material has been leached into the solution from the 2 wt% G50 starch suspension to enable formation of a lubricating surface coating. By contrast, the 0.5 wt% G50 starch suspensions at 60°C display somewhat differentiated behaviour, with the '50/50' curve displaying a characteristic shape indicative of a particle ball-bearing effect. We note that for both G50 concentrations the properties of starch granules should be identical, while the concentration of the leached starch in the solution is different. This result strongly supports the hypothesis that particle ball bearing effect is abolished by the presence of the surface film rather than by changes in the surface properties of the starch granules. We also note that changes in the suspension behaviour from 24°C to 60°C are not associated with the changes in the rheological

properties of EMIMAc-water solvents, which is taken into account by using the corresponding values of viscosity (the reference Stribeck recorded for pure EMIMAc and 60/40 EMIMAc-water solvent at 24°C to 60°C are provided in Figure 6 of Supplementary Information). Likewise the viscosity of suspensions ≤5 wt% was found to follow the Einstein equation $\left(\frac{\eta_{susp}}{\eta_0} = (1 + 2.5\varphi)\right)$ suggesting that for low suspension concentrations the granules are not aggregating and their collisions are purely elastic.

As expected, the increase in the temperature results in more partitioning of starch material and hence the lubrication even for low EMIMAc content becomes dominated by the soluble polymer.

4. Conclusions

In this work, we showed for the first time that starch polysaccharides can act as effective additives for IL lubrication. In particular, the soluble fractions of G50 starch are found to be promising candidates to facilitate lubrication of EMIMAc-water solvents, and solvent quality-responsive polymer films are formed at surfaces. We also found that starch suspension lubrication is controlled by the interplay between insoluble starch particulates (suspension-dominated friction) and dissolved starch components (polymer-dominated friction), which in turn depends on the amount of polymeric materials leached from starch in EMIMAc-water solvents. For the solvents with EMIMAc content below 60 wt%, we observed behaviour similar to that for particles in Newtonian solvents and such behaviour is explained by the entrainment of the particles into the contact (Yakubov, Branfield, Bongaerts & Stokes, 2015). With increasing EMIMAc content to 60 wt% and above, which is a favourable condition for starch polymer dissolution, a switch from the suspension-dominated lubrication to the polymer-dominated lubrication is observed.

Remarkably, the presence of very low amounts of soluble polymer (~ 0.25 wt%) completely abates particle contribution to the frictional response. We speculate that this occurs due to the formation of a lubricious polymer surface film on hydrophobic PDMS that prevents particles from being entrained into the contact. These findings may have wide implications in engineering tribology and biotribological applications, including in utilising, controlling and understanding starch and IL lubrication but also generally with regards to understanding the relative impact of suspended particles and polymers on boundary and mixed lubrication.

Acknowledgements

This work was performed in part at the Queensland node of the Australian National Fabrication Facility (ANNF-Q), a company established under the National Collaborative Research Infrastructure Strategy to provide nano- and micro-fabrication facilities for Australia's researchers. The authors thank Ms Tracey Tra Mi Ho (University of South Australia) for assistance with ellipsometric measurements; Dr Sushil Dhital, Professor Michael Gidley, Dr Torsten Witt, and Dr Fred Warren

(University of Queensland) are gratefully acknowledged for many helpful discussions. F. Xie and P. J. Halley wish to acknowledge the support of the Australian Research Council (ARC) for the research funding under the Discovery Project No. 120100344. G.E. Yakubov and J.R. Stokes wish to acknowledge the support of the Australian Research Council (ARC) for funding to the ARC Centre of Excellence in Plant Cell Walls (CE110001007).

References

Atkin, R., & Warr, G. (2007). Structure in confined room-temperature ionic liquids. *J Phys Chem C, 111*, 5162-5168.

Beattie, D. A., Harmer-Bassell, S. L., Ho, T. T. M., Krasowska, M., Ralston, J., Sellapperumage, P. M. F., & Wasik, P. (2015). Spectroscopic study of ionic liquid adsorption from solution onto gold. *Physical Chemistry Chemical Physics, 17*(6), 4199-4209.

Boehm, M. W., Shewan, H. M., Steen, J., & Stokes, J. R. (2015). Illustrating ultra-low-volume rheology on a conventional rheometer: charting the development of hyaluronan during fermentation. *Applied Rheology, in press*.

Bongaerts, J. H. H., Fourtouni, K., & Stokes, J. R. (2007). Soft-tribology: Lubrication in a compliant PDMS-PDMS contact. *Tribology International, 40*(10-12), 1531-1542.

Born, M., & Wolf, E. (1999). *Principles of optics : electromagnetic theory of propagation, interference and diffraction of light*. Cambridge; New York: Cambridge University Press.

Cave, R. A., Seabrook, S. A., Gidley, M. J., & Gilbert, R. G. (2009). Characterization of Starch by Size-Exclusion Chromatography: The Limitations Imposed by Shear Scission. *Biomacromolecules, 10*(8), 2245-2253.

Chen, P., Yu, L., Simon, G., Petinakis, E., Dean, K., & Chen, L. (2009). Morphologies and microstructures of cornstarches with different amylose-amylopectin ratios studied by confocal laser scanning microscope. *Journal of Cereal Science, 50*(2), 241-247.

Chen, P., Yu, L., Simon, G. P., Liu, X., Dean, K., & Chen, L. (2011). Internal structures and phase-transitions of starch granules during gelatinization. *Carbohydrate Polymers, 83*(4), 1975-1983.

Davies, G. A., & Stokes, J. R. (2005). On the gap error in parallel plate rheometry that arises from the presence of air when zeroing the gap. *Journal of Rheology, 49*(4), 919-922.

Davies, G. A., & Stokes, J. R. (2008). Thin film and high shear rheology of multiphase complex fluids. *Journal of Non-Newtonian Fluid Mechanics, 148*(1-3), 73-87.

Dhital, S., Shelat, K. J., Shrestha, A. K., & Gidley, M. J. (2013). Heterogeneity in maize starch granule internal architecture deduced from diffusion of fluorescent dextran probes. *Carbohydrate Polymers, 93*(2), 365-373.

Fu, Z.-q., Wang, L.-j., Li, D., Wei, Q., & Adhikari, B. (2011). Effects of high-pressure homogenization on the properties of starch-plasticizer dispersions and their films. *Carbohydrate Polymers, 86*(1), 202-207.

Gabriele, A., Spyropoulos, F., & Norton, I. T. (2010). A conceptual model for fluid gel lubrication. *Soft Matter, 6*(17), 4205-4213.

Gebbie, M. A., Valtiner, M., Banquy, X., Fox, E. T., Henderson, W. A., & Israelachvili, J. (2013). Ionic Liquids Behave as Dilute Electrolyte Solutions. *P. Natl. Acad. Sci. USA, 110*, 9674-9679.

Harvey, N. M., Yakubov, G. E., Stokes, J. R., & Klein, J. (2011). Normal and shear forces between surfaces bearing porcine gastric mucin, a high-molecular-weight glycoprotein. *Biomacromolecules, 12*(4), 1041-1050.

Horn, R., Evans, D., & Ninham, B. (1988). Double-layer and solvation forces measured in a molten salt and its mixtures with water. *J Phys Chem, 92*, 3531-3537.

Jane, J.-l. (2009). Structural features of starch granules II. In B. James & W. Roy (Eds.). *Starch (Third Edition)* (pp. 193-236). San Diego: Academic Press.

Klein, J., Zhang, X. Y., & Wilhelm, M. (2000). Biolubrication: The shear of adsorbed polyelectrolytes and of polymer brushes. *Abstracts of Papers of the American Chemical Society, 219*, U474-U474.

Kravchuk, O., & Stokes, J. R. (2013). Review of algorithms for estimating the gap error correction in narrow gap parallel plate rheology. *Journal of Rheology, 57*(2), 365-375.

Li, M., Hasjim, J., Xie, F., Halley, P. J., & Gilbert, R. G. (2014). Shear degradation of molecular, crystalline, and granular structures of starch during extrusion. *Starch - Stärke, 66*(7-8), 595-605.

Liu, W., & Budtova, T. (2012). Ionic liquid: A powerful solvent for homogeneous starch-cellulose mixing and making films with tuned morphology. *Polymer, 53*(25), 5779-5787.

Liu, W., & Budtova, T. (2013). Dissolution of unmodified waxy starch in ionic liquid and solution rheological properties. *Carbohydrate Polymers, 93*(1), 199-206.

Luallen, T. E. (2002). A Comprehensive Review of Commercial Starches and Their Potential in Foods. *Food science and technology.*(116), 757-808.

Macakova, L., Yakubov, G. E., Plunkett, M. A., & Stokes, J. R. (2010). Influence of ionic strength changes on the structure of pre-adsorbed salivary films. A response of a natural multi-component layer. *Colloids and Surfaces B-Biointerfaces, 77*(1), 31-39.

Macakova, L., Yakubov, G. E., Plunkett, M. A., & Stokes, J. R. (2011). Influence of ionic strength on the tribological properties of pre-adsorbed salivary films. *Tribology International, 44*(9), 956-962.

Mateyawa, S., Xie, D. F., Truss, R. W., Halley, P. J., Nicholson, T. M., Shamshina, J. L., Rogers, R. D., Boehm, M. W., & McNally, T. (2013). Effect of the ionic liquid 1-ethyl-3-methylimidazolium acetate on the phase transition of starch: Dissolution or gelatinization? *Carbohydrate Polymers, 94*(1), 520-530.

Min, Y., Akbulut, M., Sangoro, J. R., Kremer, F., Prud'homme, R. K., & Israelachvili, J. (2009). Measurement of forces across room temperature ionic liquids between mica surfaces. *J Phys Chem C, 113*, 16445-16449.

Nainaparampil, J. J., Eapen, K. C., Sanders, J. H., & Voevodin, A. A. (2007). Ionic-liquid lubrication of sliding MEMS contacts: Comparison of AFM liquid cell and device-level tests. *Journal of Microelectromechanical Systems, 16*(4), 836-843.

Palacio, M., & Bhushan, B. (2008). Ultrathin wear-resistant ionic liquid films for novel MEMS/NEMS applications. *Advanced Materials, 20*(6), 1194-1198.

Palacio, M., & Bhushan, B. (2010). A Review of Ionic Liquids for Green Molecular Lubrication in Nanotechnology. *Tribol. Lett., 40*, 247-268.

Pérez, S., Baldwin, P. M., & Gallant, D. J. (2009). Structural features of starch granules I. In B. James & W. Roy (Eds.). *Starch (Third Edition)* (pp. 149-192). San Diego: Academic Press.

Pérez, S., & Bertoft, E. (2010). The molecular structures of starch components and their contribution to the architecture of starch granules: a comprehensive review. *Starch/Stärke, 62*(8), 389-420.

Perkin, S. (2012). Ionic Liquids in Confined Geometries. *Phys. Chem. Chem. Phys., 2012*(14), 5052-5062.

Perkin, S., Albrecht, T., & Klein, J. (2010). Layering and shear properties of an ionic liquid, 1-ethyl-3-methylimidazolium ethylsulfate, confined to nano-films between mica surfaces *Phys. Chem. Chem. Phys., 12*, 1243-1247.

Persson, B. N. J. (2000). *Sliding friction : physical principles and applications*. Berlin ; New York: Springer.

Persson, B. N. J., & Scaraggi, M. (2009). On the transition from boundary lubrication to hydrodynamic lubrication in soft contacts. *Journal of Physics-Condensed Matter, 21*(18), 185002.

Pu, J., Jiang, D., Mo, Y., Wang, L., & Xue, Q. (2011). Micro/nano-tribological behaviors of crown-type phosphate ionic liquid ultrathin films on self-assembled monolayer modified silicon. *Surface & Coatings Technology, 205*(20), 4855-4863.

Remsing, R. C., Swatloski, R. P., Rogers, R. D., & Moyna, G. (2006). Mechanism of cellulose dissolution in the ionic liquid 1-n-butyl-3-methylimidazolium chloride: a 13 C and 35/37 Cl NMR relaxation study on model systems. *Chemical Communications*(12), 1271-1273.

Scaraggi, M., & Persson, B. N. J. (2014). Theory of viscoelastic lubrication. *Tribology International, 72*, 118-130.

Sedeva, I. G., Fornasiero, D., Ralston, J., & Beattie, D. A. (2010). Reduction of Surface Hydrophobicity Using a Stimulus-Responsive Polysaccharide. *Langmuir, 26*(20), 15865-15874.

Shogren, R. L., Fanta, G. F., & Doane, W. M. (1993). Development of starch based plastics - A reexamination of selected polymer systems in historical perspective. *Starch/Stärke, 45*(8), 276-280.

Smith, A. M., Lovelock, K. R. J., Gosvami, N. N., Licence, P., Dolan, A., Welton, T., & Perkin, S. (2012). Monolayer to Bilayer Structural Transition in Confined Pyrrolidinium-Based Ionic Liquids. *J Phys Chem Lett, 4*, 378-382.

Stokes, J. R., Davies, G. A., Macakova, L., Yakubov, G., Bongaerts, J., & Rossetti, D. (2008). From rheology to tribology: Multiscale dynamics of biofluids, food emulsions and soft matter. *Xvth International Congress on Rheology - the Society of Rheology 80Th Annual Meeting, Pts 1 and 2, 1027*, 1171-1173.

Tan, I., Flanagan, B. M., Halley, P. J., Whittaker, A. K., & Gidley, M. J. (2007). A method for estimating the nature and relative proportions of amorphous, single, and double-helical components in starch granules by C-13 CP/MAS NMR. *Biomacromolecules, 8*(3), 885-891.

Xie, F., Flanagan, B. M., Li, M., Sangwan, P., Truss, R. W., Halley, P. J., Strounina, E. V., Whittaker, A. K., Gidley, M. J., Dean, K. M., Shamshina, J. L., Rogers, R. D., & McNally, T. (2014). Characteristics of starch-based films plasticised by glycerol and by the ionic liquid 1-ethyl-3-methylimidazolium acetate: A comparative study. *Carbohydrate Polymers, 111*, 841-848.

Yakubov, G. E., Branfield, T. E., Bongaerts, J. H. H., & Stokes, J. R. (2015). Tribology of particle suspensions in rolling-sliding soft contacts. *Biotribology, in press*.

Yakubov, G. E., Macakova, L., Wilson, S., Windust, J. H. C., & Stokes, J. R. (2015). Aqueous lubrication by fractionated salivary proteins: Synergistic interaction of mucin polymer brush with low molecular weight macromolecules. *Tribology International, 89,* 34-45.

Zhang, B., Chen, L., Xie, F., Li, X., Truss, R. W., Halley, P. J., Shamshina, J. L., Rogers, R. D., & McNally, T. (2015). Understanding the structural disorganization of starch in water-ionic liquid solutions. *Physical Chemistry Chemical Physics, 17,* 13860-13871.

Zhang, C., Liu, R., Xiang, J., Kang, H., Liu, Z., & Huang, Y. (2014). Dissolution Mechanism of Cellulose in N, N-Dimethylacetamide/Lithium Chloride: Revisiting through Molecular Interactions. *The Journal of Physical Chemistry B, 118,* 9507−9514.

Figure 5. (A) Relative friction coefficient, μ_r, of 0.25% G50 starch solutions in different EMIMAc-water solvents. The relative friction coefficient is expressed relative to either water or pure EMIMAc-water mixture. (B) Time-dependency of friction coefficient for 0.25 wt% G50 starch solutions in various EMIMAc-water solvents. All measurements are performed at constant speed of 5 mm/s.

Starch	**Solvent**	**Solute**	**Concentration**	$\mu_{r(H2O)}$	$\mu_{r(solvent)}$
G50	50/50	'65/35' extracted	0.25%	0.49 ± 0.03	0.52 ± 0.03
G50	55/45	'65/35' extracted	0.25%	0.41 ± 0.02	0.48 ± 0.02
G50	60/40	'65/35' extracted	0.25%	0.40 ± 0.02	0.48 ± 0.02
G50	65/35	'65/35' extracted	0.25%	0.38 ± 0.01	0.53 ± 0.01
G50	65/35	'65/35' extracted	0.33%	0.32 ± 0.00	0.44 ± 0.00
G50	70/30	'65/35' extracted	0.25%	0.34 ± 0.01	0.78 ± 0.01
WMS	65/35	'65/35' extracted	0.25%	0.62 ± 0.04	0.84 ± 0.04
WMS	65/35	'65/35' extracted	0.33%	0.57 ± 0.03	0.78 ± 0.03

Table 1. Relative friction coefficients, μ_r, of starch solutions in different EMIMAc-water solvents; the relative friction coefficients are expressed relative to either water or pure EMIMAc-water solvents. All soluble starch materials were extracted into 65/35 EMIMAc/water solvent. All measurements are performed at constant speed of 5 mm/s.

Starch	**Solvent**	**Solute**	**Concentration**	$\mu_{r(H2O)}$	$\mu_{r(solvent)}$
G50	50/50	'50/50' extracted	0.008%	0.80 ± 0.02	0.86 ± 0.02
G50	65/35	'50/50' extracted	0.008%	0.59 ± 0.03	0.80 ± 0.03
G50	50/50	'65/35' extracted	0.225%	0.81 ± 0.03	0.87 ± 0.03
G50	65/35	'65/35' extracted	0.225%	0.39 ± 0.02	0.55 ± 0.02

Table 2. (A) Relative friction coefficient, μ_r, of starch solutions for four different combinations of solvents. All measurements are performed at constant speed of 5 mm/s